Received 16 June 2023; accepted 3 July 2023. Date of publication 19 July 2023; date of current version 15 August 2023.

Digital Object Identifier 10.1109/OJAP.2023.3296582

Dual-Port RHCP Compact Antenna at 868 MHz Using a 120° Hybrid Coupler

FABIEN FERRERO[1] (Member, IEEE), AND LE HUY TRINH[2] (Member, IEEE)

[1]Université Cote d'Azur, CNRS, LEAT, 06903 Sophia-Antipolis, France

[2]University of Information Technology, Vietnam National University Ho Chi Minh City, Ho Chi Minh City 71308, Vietnam

CORRESPONDING AUTHOR: F. FERRERO (e-mail: fabien.ferrero@univ-cotedazur.fr)

This work was supported in part by the Vietnam National University HoChiMinh City (VNU-HCM) under Grant C2023-26-01, and in part by the French Government under Grant ANR-15-IDEX-01.

ABSTRACT This work presents the design of a compact dual-port circularly polarized antenna based on the new coupler topology. The antenna can radiate a right-hand circular polarization (RHCP) in two opposite directions depending on the input port. In the proposed structure, the radiating system has three inverted F antennas connected to a 120° hybrid coupler. The modeling and design of the 5-ports hybrid coupler are described and experimentally validated. The antenna prototype is fabricated using two 1.6mm-thick low-cost FR4 Epoxy substrates assembled with metal wires, with a dimension of 80mm × 80mm × 12mm (ka < 0.74). The proposed antenna provides the realized RHCP gain of 2.4 dBic and 1.8dBic at 868 MHz for Port 1 and Port 2, respectively.

INDEX TERMS Circular polarization, coupler, antennas.

I. INTRODUCTION

IN IN the last decade, Low Power Wide Area Network (LPWAN) technology came out as a perfect choice for enabling longer-range connections thanks to its efficient power consumption and low cost. The number of connected objects is expected to reach 41.6 billion in 2025 [1] raising the challenge of massive connectivity at the heart of the Internet of Things (IoT) paradigm. The compactness and antenna integration is also strong requirement for the IoT terminal [2], especially when low-frequency bands like 868/915 MHz ISM are targeted. In several studies, the circularly polarized (CP) antennas are mentioned to reduce the dependence on the device orientation and improve the communication quality [3] needed for LP-WAN applications. In addition, multi-port antenna with orthogonal radiation patterns are needed for Multiple Input Multiple Output (MIMO) communications [4]. Designing an antenna gathering all the above criteria is a considerable challenge. Multi-port antennas with CP modes have been reported using different technologies. Quadrature hybrid coupler is a classical solution to provide a left and right-hand CP [5], [6], [7]. A solution based on loading modified slot feeding structure below a metasurface has shown a very low profile structure [8]. A field transformation method with a dual-linear feed patch was demonstrated with a wideband axial ratio characteristic [9]. However, all these techniques have a limitation on the total electrical size, which is large with $ka > 1$ ($k = 2\pi/\lambda_0$ and a is the radius of the smallest sphere that completely encloses the entire antenna system). Recently, Wu et al. [10] proposed an electrically small Huygens dipole antenna with dual-port CP modes with ka < 1. A complex feeding system using a complex eight substrate layers structure is required, making this solution not optimal for low-cost IoT applications.

Recently, the use of triple feed configuration with sequential phase shift using three miniature Inverted F Antenna to generate CP has been studied and shown optimal properties for CP antenna miniaturization [11], [12]. Similarly to a Huygens source, this triple feed configuration radiates a right-hand CP pattern in only one hemisphere. In case of terminal misalignment, the capability to radiate in the opposite hemisphere would increase the robustness of the communication link. In order to provide the capability to radiate RHCP in two opposite directions, a triple IFA structure should be fed in a clockwise or counter-clockwise 120° sequentially phase shift. Hybrid microwave couplers were introduced in the 1940s as a development of hybrid coils [13]. This terminology refers to the component's

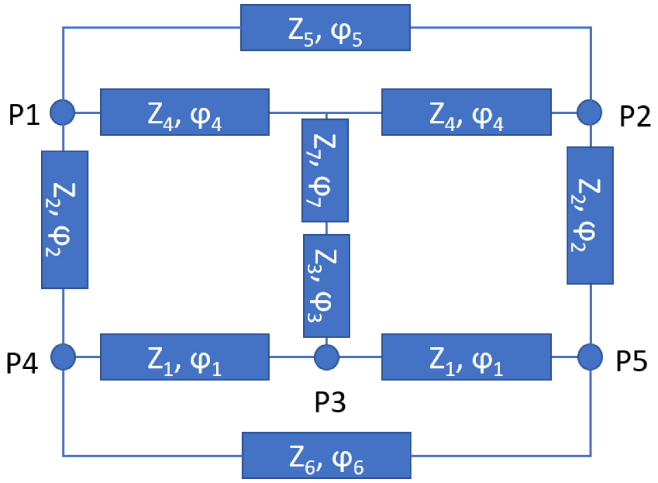

FIGURE 1. 120° ideal Hybrid coupler proposed circuit.

functionality, where the input signal from a particular port is coupled to some ports and isolated from others. The concept of 120° hybrid coupler has been proposed in the optical domain based on the polarization splitter and rotator [14]. The development at lower frequency has only been reported in [15] to feed a patch antenna at 5.8GHz without any description of the coupler. To the best of our knowledge, the complete study and comprehensive design of a 120° has never been considered in the open literature.

This paper studies a 5 ports 120° hybrid coupler from the theoretical transmission line topology to a practical implementation in Section II. In Section III, the 120° coupler is then connected to a trifilar antenna structure resonating at 868 MHz to provide a dual-port antenna with the capability to radiate an RHCP pattern in two opposite directions. The prototyping and measurements are reported in Section IV, and a comparison with state-of-the-art is proposed in Section V.

II. DESIGN OF A 120° HYBRID COUPLER

A 120° coupler based on an ideal transmission line is shown in Fig. 1. The circuit structure consists of five 50 Ω ports and ten transmission lines. In general, it is designed to be symmetrical about the vertical axis. The input signals from Port 1 or Port 2 are divided into three paths to Port 3, 4, and 5 with an equi-amplitude level. Moreover, a 120° sequential phase shift clockwise (Port 1) or counterclockwise (Port 2) is obtained among the three output ports depending on the input port used. The optimized transmission lines parameters (characteristic impedance and phase delay) have been computed using ADS microwave simulator and are given in Table 1.

The full S-parameters for Port 1 are presented with dB scale value in Fig. 2. The transmitted phase value to Ports 3, 4, and 5 are presented in Fig. 3 from Port 1 and Port 2, respectively. According to this result, the ideal S-matrix can be extracted. As observed, Port 1 and 2 have an isolation

TABLE 1. 120° hybrid coupler transmission line parameters.

Line	Char. Impedance	Z(■)	Phase delay	Φ (°)
L1	Z1	30	$\phi 1$	120
L2	Z2	45	$\phi 2$	90
L3	Z3	140	$\phi 3$	10
L4	Z4	36	$\phi 4$	120
L5	Z5	250	$\phi 5$	67
L6	Z6	62	$\phi 6$	113
L7	Z7	25	$\phi 7$	51

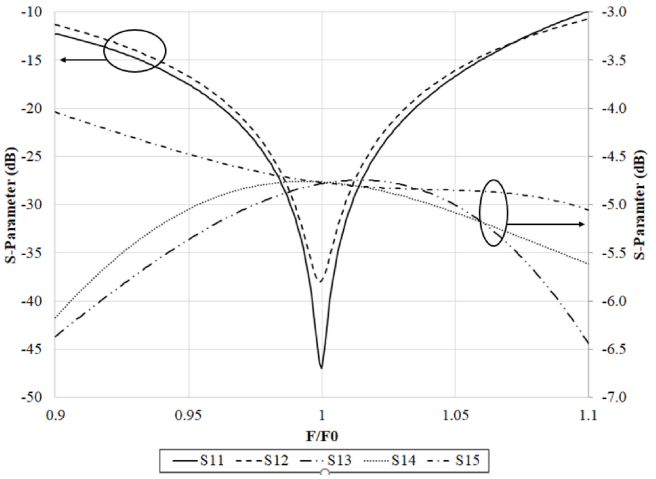

FIGURE 2. Simulated S-Parameters in dB scale for ideal 120° hybrid coupler with normalized frequency.

higher than $30dB$, and power is equally transferred to Port 3, 4, and 5 ($-4.77dB$ coupling). A sequential 120° phase shift is obtained clockwise (Port 1) and counterclockwise (Port 2) as predicted.

$$S = \frac{1}{\sqrt{(3)}} \begin{bmatrix} 0 & 0 & e^{-j\frac{2}{3}\pi} & e^{j\frac{2}{3}\pi} & 1 \\ 0 & 0 & 1 & e^{j\frac{2}{3}\pi} & e^{-j\frac{2}{3}\pi} \\ e^{-j\frac{2}{3}\pi} & 1 & -\frac{1}{\sqrt{(3)}} & -\frac{1}{\sqrt{(3)}} & -\frac{1}{\sqrt{(3)}} \\ e^{j\frac{2}{3}\pi} & e^{j\frac{2}{3}\pi} & -\frac{1}{\sqrt{(3)}} & -\frac{1}{\sqrt{(3)}} & -\frac{1}{\sqrt{(3)}} \\ 1 & e^{-j\frac{2}{3}\pi} & -\frac{1}{\sqrt{(3)}} & -\frac{1}{\sqrt{(3)}} & -\frac{1}{\sqrt{(3)}} \end{bmatrix} \quad (1)$$

III. CIRCULAR POLARIZED DUAL-PORT ANTENNA DESIGN

A. RADIATING STRUCTURE

In order to radiate a circularly polarized wave, the tri-fillar structure presented in [12] is used. From the study [16], it is possible to conclude that an 80 mm diameter and 12 mm height structure is providing a good trade-off between compactness, isolation between antennas, and Right Hand Circularly Polarized (RHCP) gain. The radiation structure is composed of three identical radiating elements placed around a central axis. The radiating structures are the vertical Inverted F Antenna (IFA) built using two substrates as shown in Fig. 4. The orientation of the IFA will

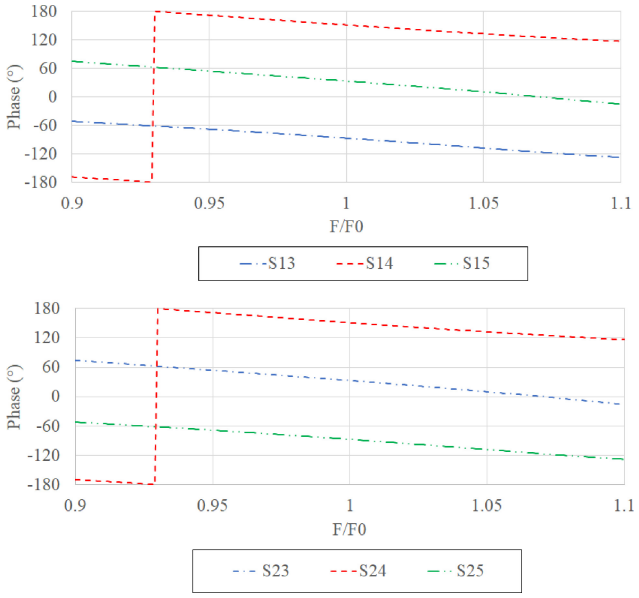

FIGURE 3. Simulated S-Parameters phase for ideal 120° hybrid coupler.

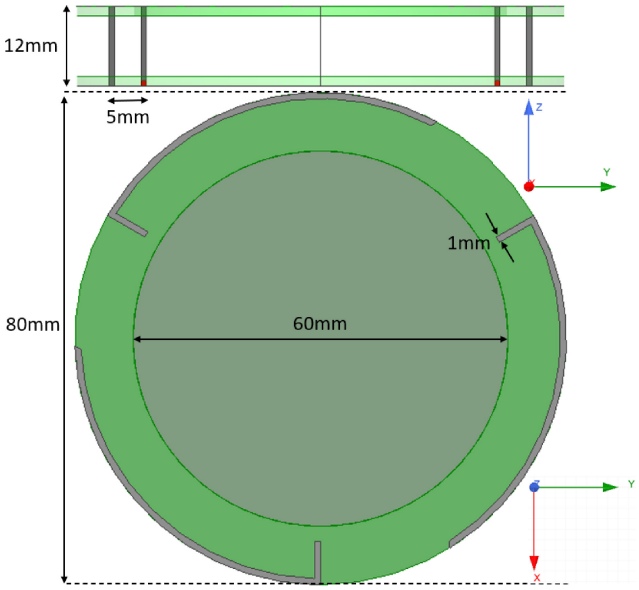

FIGURE 4. Front and Top view of the three filar antenna structure.

define the direction of the current and the sense of circular polarization (left or right). For RHCP, IFAs have to be wrapped around the ground plane as shown in Fig. 4. In order to facilitate the prototype assembly, the ground plane and antenna are printed on two 1.6 mm-thick substrates ($\epsilon_r = 4.4$) connected by vertical metal wires. The antenna dimensions are optimized to obtain a -15 dB matching at 868 MHz. With a clockwise equi-amplitude 120° feeding, the structure radiate a RHCP pattern toward $+z$ direction. In case of a counterclockwise equi-amplitude 120° feeding, the RHCP radiation is oriented toward $-z$ direction.

The feeding circuit is integrated within the antenna structure in the next step.

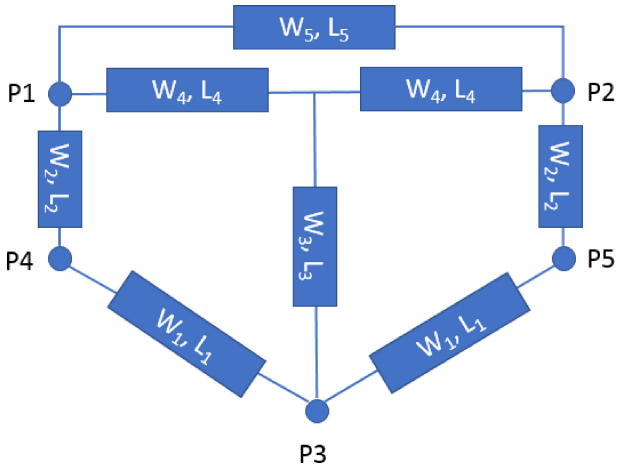

FIGURE 5. Simplified structure of 120° Hybrid coupler circuit.

TABLE 2. Microstrip line width and length on a 1.6mm-thick substrate with $\epsilon_r = 4.4$.

	Width	mm	Length	mm
MSL 1	W_1	3	L_1	57
MSL 2	W_2	3	L_2	55
MSL 3	W_3	1.44	L_3	34
MSL 4	W_4	2.63	L_4	64
MSL 5	W_5	0.3	L_5	52

B. SIMPLIFIED IMPLEMENTATION OF A 120° COUPLER

In this section, the ideal 120° coupler circuit is modified to be fabricated on a double-layer substrate using microstrip lines. In order to simplify and avoid the crossing line: line N°6 is removed, and lines 3 and 7 are unified into a single line as shown in Fig. 5. After optimizing the structure for a 1.6mm-thick FR4 substrate ($\epsilon_r = 4.4$ and $\tan\delta = 0.02$), the width and length parameter for each line is given in mm in Table 2. The simplified solution provides sufficient matching and isolation ($> 15dB$) for proper operation.

The 120° coupler is implemented on an 80mm-diameter disk, as shown in Fig. 6 to fit with the antenna system. The lines are generally folded to keep them in a compact area. Port 3, 4, 5 are evenly distributed 120° around the center of the disk, to be easily connected with the radiating elements at the top board via the metal wires. The structure is optimized by using ANSYS Full-wave solver.

S-parameter results for the coupler are reported in Fig. 7 with a good agreement between simulation and measurement. At 868 MHz, Port 1 reflection coefficient is lower than -15 dB, and the isolation between Port 1 and Port 2 is lower than -17 dB. Moreover, the signal from Port 1 is almost evenly distributed to Port 3, 4, and 5, with the insertion loss ranging from -5.2 dB to -5.6 dB. Besides, the simulated and measured phases are presented in Fig. 8. According to these results, the phase shifts between the ports are about 122°, 122°, and 116° for Port 4 to Port 3, Port 3 to Port 5, and Port 5 to Port 4, respectively. Thanks to the vertical symmetry, results for Port 2 are identical with counterclockwise phase shift distribution.

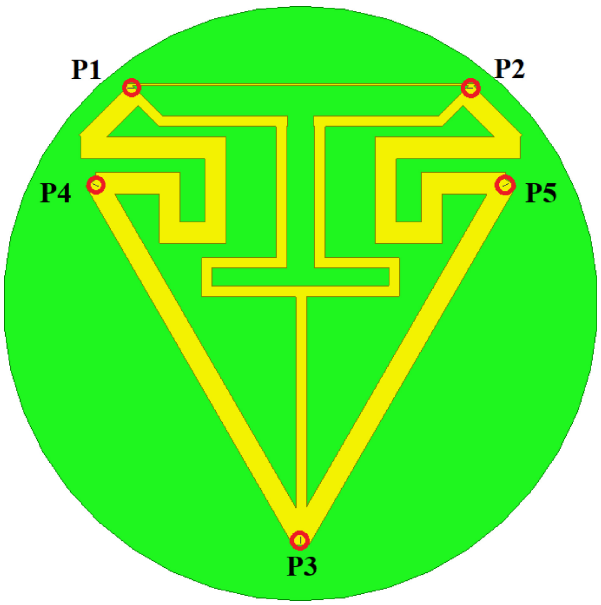

FIGURE 6. Top View of the feeding circuit with antennas.

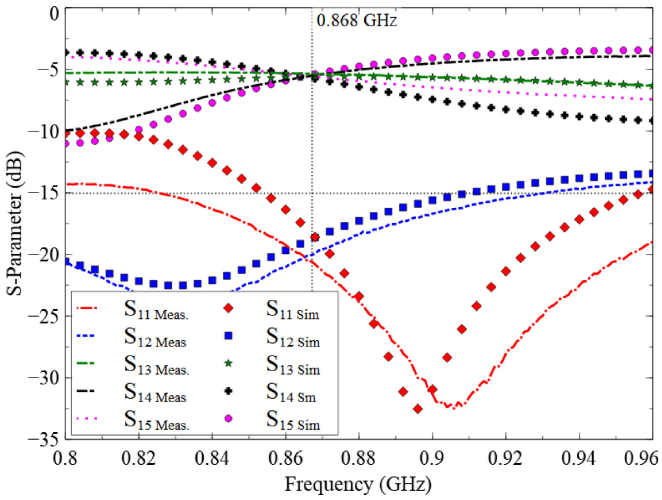

FIGURE 7. Simulated and measured S-Parameters in dB scale for 120° hybrid coupler.

C. DUAL-PORT RHCP ANTENNA STRUCTURE

After combining the 120° hybrid coupler with the radiating elements, the final structure is shown in Fig. 9. Three IFA feeds are connected with Port 3, 4, 5 using 1mm-thick metal wires, while the shorts are directly soldered to the ground at the bottom layer of the coupler board. Port 1 or 2 can be used to feed the three IFA with clockwise or counterclockwise phase distribution. The simulated S-Parameter results are reported in Fig.10. Reflection coefficient on Port 1 and Port 2 and isolation among them are lower than −15 dB at 868 MHz.

The simulated radiation parameters versus frequency are shown in Fig. 11 for Port 1 and Port 2. A peak directivity of 4.5 dBi is obtained at 868 MHz, which justifies the wide angular beamwidth (110°) compared with a patch antenna. By feeding Port 1, the RHCP gain for $\theta = 0°$

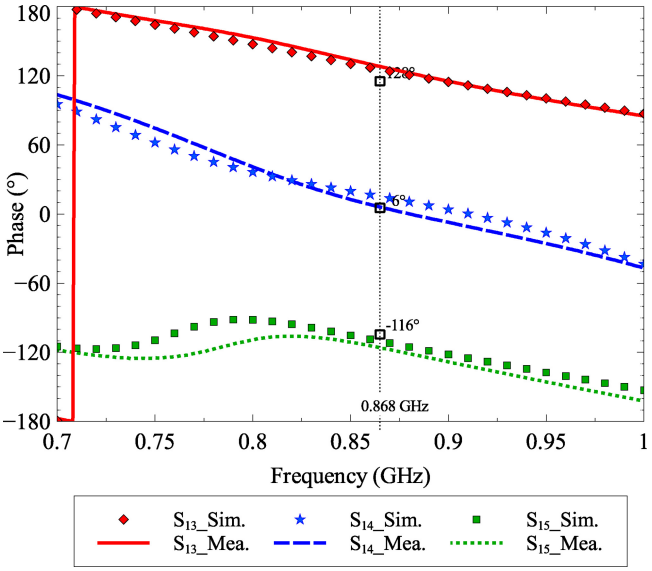

FIGURE 8. Simulated and measured S-Parameters Phase for 120° hybrid coupler.

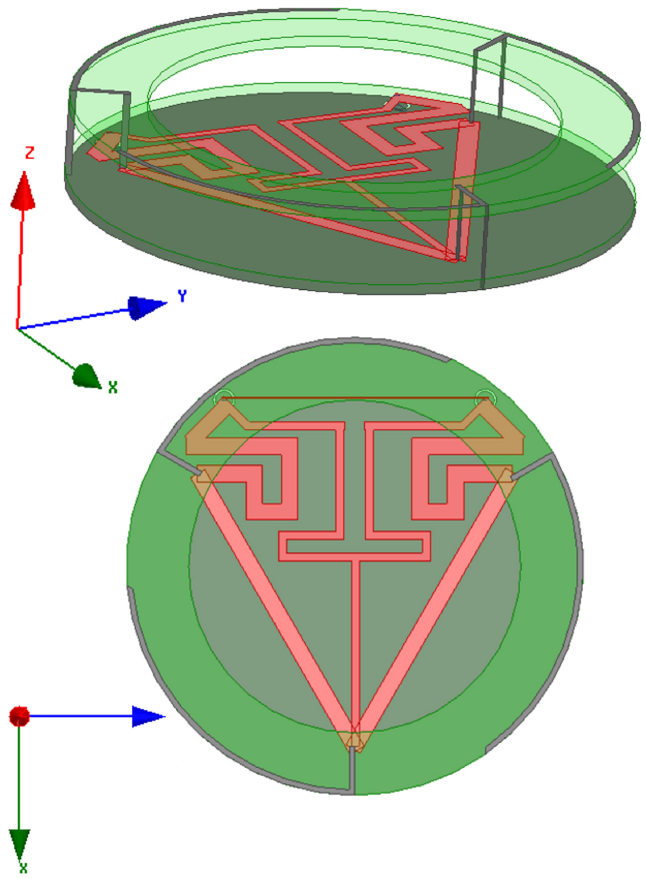

FIGURE 9. Dual-port RHCP antenna structure.

reach 2.5 dBic with an axial ratio lower than 1.4 dB at 868 MHz. The same RHCP gain is obtained by feeding Port 2 in $\theta = 180°$ direction with a 0.4 dB axial ratio. A total efficiency of 65% (−1.9 dB) is obtained at 868 MHz for both ports. As shown in Table 3, substrate

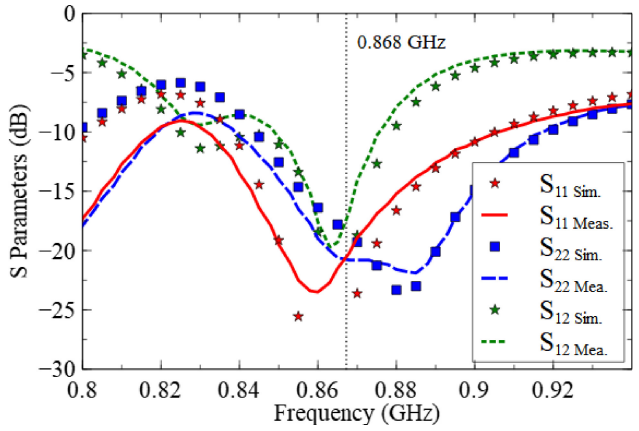

FIGURE 10. Simulated and measured S-Parameter results of dual-port CP antenna.

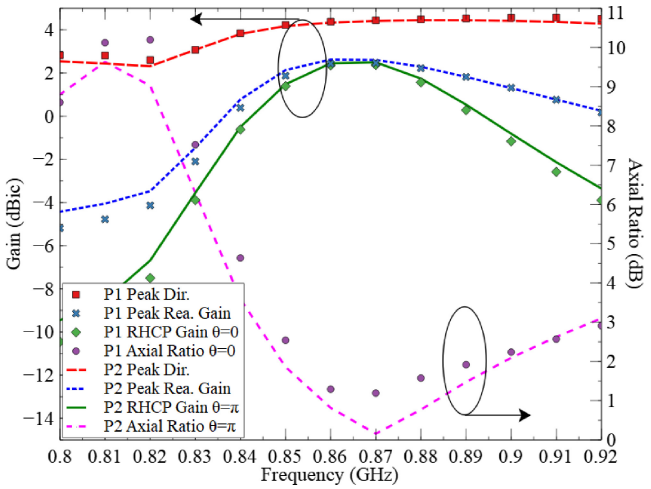

FIGURE 11. Simulated peak directivity and gain, RHCP gain and axial ratio versus frequency for Port 1 and 2.

TABLE 3. Effect of substrate tanδ on antenna performances at 868*MHz*.

Substrate tanδ	0.005		0.02	
Port number	1	2	1	2
Tot. Efficiency (dB)	-0.86	-0.87	-1.94	-1.86
Peak Tot. IEEE Gain (dBi)	3.63	3.66	2.63	2.76
Peak Tot. Real. Gain (dBi)	3.61	3.57	2.46	2.54
Peak Real. RHCP Gain (dBic)	3.54	3.53	2.39	2.46

dielectric loss has a large impact on antenna performance. Total efficiency is reduced by more than 1dB if a low-cost FR4 substrate (tanδ = 0.02) is used in place of a low-loss substrate with equivalent permittivity (tanδ = 0.005). Simulated radiation patterns at 868 MHz show a 123° beamwidth in $\theta = 0°$ direction for Port 1 (Fig. 14(a) and 122° beamwidth in $\theta = 180°$ direction for Port 2 (Fig. 14(b).

IV. PROTOTYPING AND MEASUREMENTS

A. PROTOTYPE FABRICATION

The proposed concept is fabricated on a 1.6mm-thick FR4 Epoxy with the $\epsilon_r = 4.4$ and $tan\delta = 0.02$. The FR4 higher loss substrate is selected with the knowledge of the facts, in order to meet the low-cost IoT requirement. The two substrates are assembled by soldering six 1mm-thick copper wires, making the structure mechanically robust. A picture of the front and back view of the proposed antenna is shown in Fig. 12. The blue solder mask was removed above the coupler copper trace for aesthetic reasons. Two SMA connectors are soldered on the bottom layer with the signal pin connected to Port 1 and Port 2, respectively.

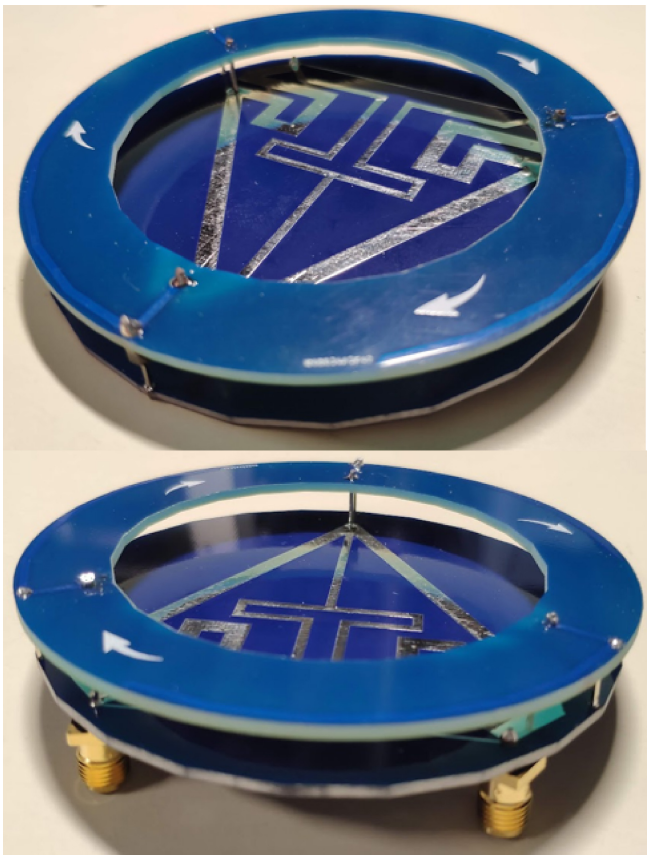

FIGURE 12. Prototype front and back view.

B. ANTENNA MEASUREMENTS

The S parameters of the prototype are measured and compared with the simulation results in Fig. 10. It shows a fair agreement considering the complexity of the structure. Considering a −10 dB reflection coefficient and isolation criteria, the proposed antenna has a 29 MHz impedance bandwidth from 848 MHz to 877 MHz. The isolation between Port 1 and Port 2 is better than −17 dB at 868 MHz.

The radiation pattern characteristics are measured with a near-field Satimo StarLab station with ferrite beads connected to the feeding cable in order to limit the current flowing on the cable shield. Port 1 and Port 2 are measured independently with the second port loaded with 50 Ohm. The measured results versus frequency are presented in Fig. 13. The antenna has a total efficiency of −1.98dB for port 1 and

TABLE 4. Comparison of the dual port CP antennas reported in the literature.

Ref.	ka	FBW (%)	RG (dBic)	FTBR (dB)	isolation (dB)	electrical size ($\lambda_0{}^3$)	Sub. tanδ
[6]	2.12	4	6	30	> 15	$0.5 \times 0.5 \times 0.057 = 0.0143$	0.002
[8]	3.17	31.3	7	18	> 10	$0.71 \times 0.71 \times 0.04 = 0.0202$	0.0027
[10]	0.94	0.99	1.81	4.1	> 15.6	$\pi \times 0.15^2 \times 0.053 = 0.0037$	0.005
This work	**0.74**	3.36	2.4	6.1	> 17.2	$\pi \times 0.12^2 \times 0.035 = 0.0015$	0.02

* λ_0 *is the wavelength at the center frequency.* *FBW is defined as the fractional bandwidth with* $|S_{11}|_{dB}$, $|S_{22}|_{dB}$, *and* $|S_{21}|_{dB}$ *lower than -10dB*

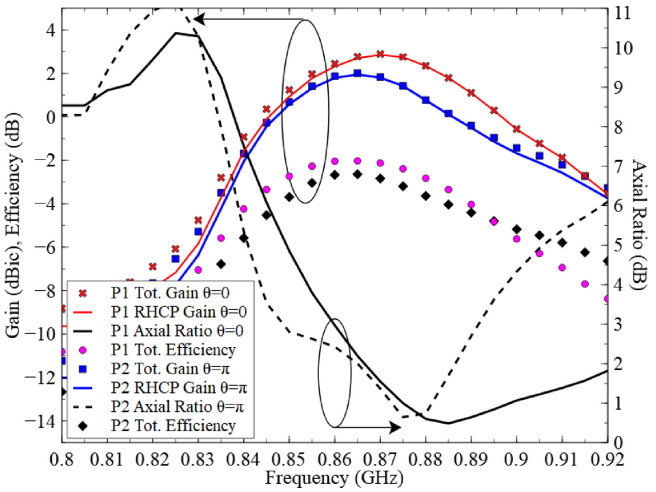

FIGURE 13. Measured total efficiency, total IEEE gain, RHCP gain, and axial ratio versus Frequency for Port 1 and 2.

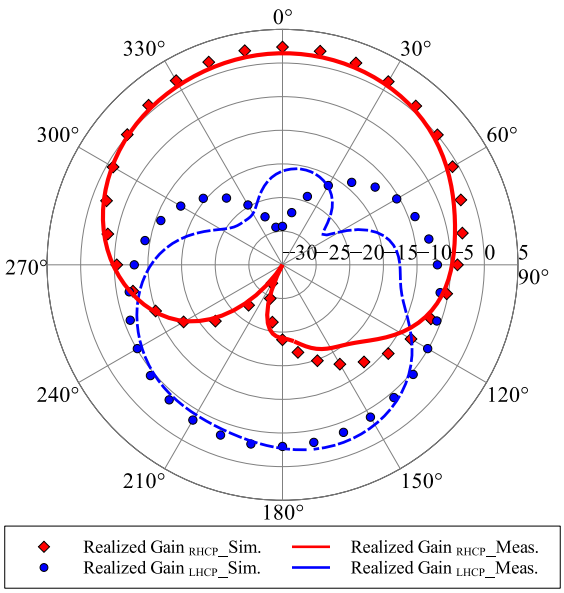

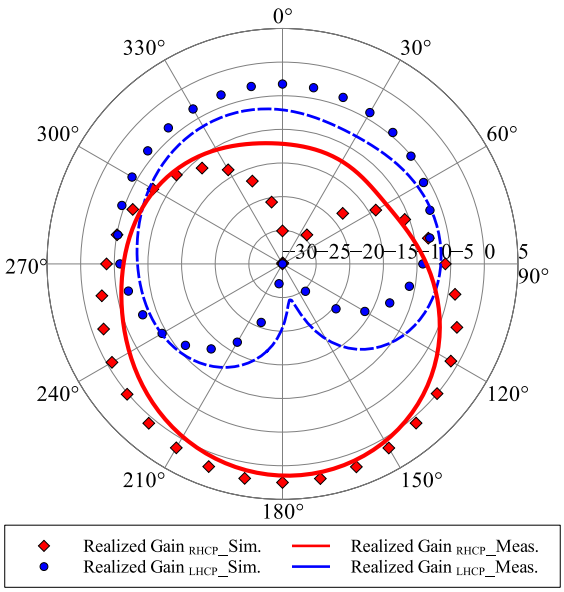

FIGURE 14. Simulated and measured radiation pattern at 868 MHz using (a) Port 1 with Port 2 matched (b) Port 2 with Port 1 matched.

−2.64dB at 868 MHz. The lower performance on port 2 can be explained by the connector and cable effect. As shown in Fig. 12, the RHCP pattern is oriented in the direction of the SMA connectors.

Using Port 1, the prototype radiates a 2.4dBic RHCP gain at 868 MHz in $\theta = 0°$ direction with a 1.4 dB axial ratio. With Port 2, a 1.8 dBic RHCP gain is measured in $\theta = 180°$ with an axial ratio of 1.1 dB.

Finally, the radiation patterns at 868 MHz are presented for Port 1 on Fig. 14(a) and Port 2 on Fig. 14(b). It confirms that a 120 ° −3dB RHCP beamwidth is obtained for Port 1. At Port 2, a –3dB RHCP beamwidth of 87 ° is measured. The decrease can be attributed to the effect of connectors and measurement cables.

V. COMPARISON WITH STATE OF THE ART AND CONCLUSION

In this paper, a 120° hybrid coupler has been successfully analyzed, designed, and measured. A comparison with similar works is reported in the literature and is shown in Table 4. The proposed work is much smaller than [6], [8] and provide better performance in terms of realized gain (RG), fractional bandwidth (FBW), front-to-back ratio (FTBW) and isolation compared to [10] for similar size. It can also be noted that the structure is realized using a higher loss substrate compared with SoA. The dual-radiation RHCP pattern using 120° coupler has been demonstrated and confirmed the effectiveness of such approach for antenna miniaturization on low-cost FR4 substrate. With 63% of total efficiency at 868 MHz, the proposed structure is suitable for LPWAN application. In the future, the ideal 120° coupler can be implemented on a multi-layer PCB in order to optimize matching and isolation.

ACKNOWLEDGMENT

The CREMANT, joint lab between UCA and Orange, is acknowledged for its support in radiation measurements. They would like to thanks Peter Ibelings for the great discussion about 120° hybrid couplers.

REFERENCES

[1] "Worldwide global datasphere IoT device and data forecast, 2019–2023," Int. Data Corp., Framingham, MA, USA, U.S. Patent 45 066 919, Jun. 18, 2019.
[2] H. Wong, K. Luk, C. H. Chan, Q. Xue, K. K. So, and H. W. Lai, "Small antennas in wireless communications," *Proc. IEEE*, vol. 100, no. 7, pp. 2109–2121, Jul. 2012.
[3] S. S. Gao, Q. Luo, and F. Zhu, "Introduction to circularly polarized antennas," in *Proc. Circul. Polarized Antennas*, 2014, pp. 1–28, doi: 10.1002/9781118790526.ch1.
[4] C. A. Balanis, "Antenna design considerations for MIMO and diversity systems," in *Modern Antenna Handbook*. New York, NY, USA: Wiley, 2008, pp. 1327–1375, doi: 10.1002/9780470294154.ch26.
[5] L. Wen, S. Gao, Q. Luo, W. Hu, and B. Sanz-Izquierdo, "Design of a wideband dual-feed circularly polarized antenna for different axial ratio requirements," *IEEE Antennas Wireless Propag. Lett.*, vol. 20, no. 1, pp. 88–92, Jan. 2021, doi: 10.1109/LAWP.2020.3041362.
[6] R. Ferreira, J. Joubert, and J. W. Odendaal, "A compact dual-circularly polarized cavity-backed ring-slot antenna," IEEE Trans. Antennas Propag., vol. 65, no. 1, pp. 364–368, Jan. 2017, doi: 10.1109/TAP.2016.2623654.
[7] X. Lin and Z. Xie, "A compact dual-band dual circularly polarized aperture-coupled patch antenna for RFID application," in *Proc. IEEE 5th Asia-Pac. Conf. Antennas Propag. (APCAP)*, 2016, pp. 55–56, doi: 10.1109/APCAP.2016.7843096.
[8] S. Liu, D. Yang, and J. Pan, "A low-profile broadband dual-circularly-polarized metasurface antenna," *IEEE Antennas Wireless Propag. Lett.*, vol. 18, no. 7, pp. 1395–1399, Jul. 2019, doi: 10.1109/LAWP.2019.2917758.
[9] H. Shi, H. Giddens, and Y. Hao, "Dual-circularly polarized patch antenna using field transformation medium," *IEEE Antennas Wireless Propag. Lett.*, vol. 16, pp. 2869–2872, 2017, doi: 10.1109/LAWP.2017.2750618.
[10] Z. Wu, M.-C. Tang, T. Shi, and R. W. Ziolkowski, "Two-port, dual-circularly polarized, low-profile broadside-radiating electrically small huygens dipole antenna," *IEEE Trans. Antennas Propag.*, vol. 69, no. 1, pp. 514–519, Jan. 2021.
[11] L. H. Trinh, K. T. Lu, M. T. Nguyen, N. V. Truong, and F. Ferrero, "Miniature circularly polarized antenna for UHF RFID handheld reader: Design and experiments," *Progr. Electromagn. Res. M*, vol. 93, pp. 43–52, Jun. 2020, doi: 10.2528/PIERM20041004.
[12] L. H. Trinh, N. Vu Truong, and F. Ferrero, "Low cost circularly polarized antenna for IoT space applications," *Electronics*, vol. 9, no. 10, p. 1564, 2020.
[13] W. A. Tyrrell, "Hybrid circuits for microwaves," *Proc. IRE*, vol. 35, no. 11, pp. 1294–1306, Nov. 1947.
[14] M. Saber et al., "Demonstration of a 120° hybrid based simplified coherent receiver on SOI for high speed PON applications," *Opt. Exp.*, vol. 26, no. 24, pp. 31222–31232, 2018.
[15] M. Baert, "Triple feed patch antenna," Feb. 5, 2019. Accessed: Dec. 13, 2021. [Online]. Available: https://www.maartenbaert.be/quadcopters/antennas/triple-feed-patch-antenna/
[16] M. T. Nguyen, L. H. Trinh, and F. Ferrero, "Impact of miniaturization on a UHF tri-fillar antenna for IoT communication from satellite," in *Proc. IEEE APS Symp.*, Montréal, QC, Canada, 2020, pp. 403–404.

FABIEN FERRERO (Member, IEEE) received the Ph.D. degree in electrical engineering from the University of Nice-Sophia Antipolis in 2007. From 2008 to 2009, he worked for IMRA Europe (Aisin Seiki Research Center) as a Research Engineer and developed automotive antennas. In 2010, he is recruited as an Associate Professor with the Polytechnic School, Université Nice Sophia-Antipolis. Since 2018, he has been a Full Professor with the Université Côte d'Azur. He is doing his research with the Laboratoire d'Electronique, Antennes et Telecommunications. His studies concerned the design and measurement of millimetric antennas, IoT systems, and space applications.

LE-HUY TRINH (Member, IEEE) was born in Quy Nhon, Vietnam, in 1988. He received the M.S. degree in electronics engineering and the Ph.D. degree from the University of Nice Sophia Antipolis, Nice, in 2012 and 2015, respectively.

Since 2015, he has been a Lecturer with the University of Information and Technology, Vietnam National University Ho Chi Minh City, Vietnam. His current research interest includes the miniature, reconfigurable and multi-standards antennas, especially for low power wide area networks and Internet-of-Things applications. During the Ph.D. degree, he has been participated the SPECTRA Project that received the Excellence Award in the category "Network Technologies." In this project, he design a multiple multiband antenna using for 4G end device.